

## **SUPPLEMENTARY METHODS**

### **Animals**

For all experiments, adult male Long-Evans rats (P60 upon arrival, Envigo Laboratories, Indianapolis, IN) were individually housed in standard polycarbonate cages measuring 19"x10.5"x8". Housing facilities were controlled for temperature (68-72 °F) and humidity (45-55%). Rats were singly housed for the duration of each experiment – a time frame that ranged from 50-200 days depending on the manipulation (i.e., anatomy experiments required shorter duration than behavioral experiments).

### **Stereotaxic surgery**

Rats undergoing stereotaxic surgery were induced and maintained under a surgical plane of anesthesia using isoflurane (1-5%). Surgeries were performed on a rat stereotaxic instrument (Kopf Instruments, Tujunga, CA, USA). Intracranial injections were made with back-filled custom glass pipettes with a tip diameter of  $50 \pm 10 \mu\text{m}$  connected to a nanojector (Drummond Scientific Company, Broomall, PA, USA) or a 2  $\mu\text{L}$  syringe (Model 7002, Hamilton Company, Reno, NV, USA) operated using a motorized pump (WPI, Inc, Sarasota, FL, USA). For tract tracing experiments, 100 nL 0.5% Cholera toxin B (CtB; Sigma Aldrich, St Louis, MO, USA) or 200 nL green fluorescent retrobeads (Lumafuor, Durham, NC, USA) were unilaterally injected into the RMTg (AP: -7.3; ML: +1.4; DV: -8.0 from skull; 6° lateral) at a rate of ~30 nL/s. For optogenetics experiments, rats were unilaterally injected with 500 nL of AAV2-hSyn-hChR2-(H134R)-eYFP-WPRE-pA ( $3.9 \times 10^{12}$  mol/mL; UNC Vector Core, Chapel Hill, NC, USA) into the dmPFC (AP: +3.2; ML:  $\pm 0.6$ ; DV: -3.5 from skull) or lateral habenula (LHb; AP: -3.6; ML:  $\pm 1.2$ ; DV: -4.1 from dura; 6° lateral) at a rate of 1-3 nL/s. During the same surgery, rats were implanted with a custom-made 200  $\mu\text{m}$  optic fiber implant targeting either the RMTg (AP: -7.3; ML:  $\pm 2.1$ ; DV: -7.9 from skull; 10° lateral) or VTA (AP: -5.6; ML:  $\pm 1.4$ ; DV: -7.8 from skull; 6° lateral). Implants were secured with dental cement. An intersectional, dual-virus approach was used to investigate the extent of

dmPFC-RMTg collateralization and structural plasticity in dmPFC-RMTg neurons following exposure to aversive stimuli. For these experiments, rats were unilaterally injected with 500 nL of either AAVretro-Cre ( $\geq 7.0 \times 10^{12}$  GC/mL; gift from Janelia Farms, Ashburn VA, US) or AAV2retro-pmSyn1-EBFP-Cre ( $1.1 \times 10^{13}$  GC/mL; Addgene, Watertown, MA, USA) into the RMTg (AP: -7.3; ML: +1.4; DV: -8.0 from skull; 6° lateral) and 500 nL of AAV8.2-hEF1alpha-DIO-SYP-EYFP ( $2.19 \times 10^{13}$  vg/mL; Rachel Neve, MIT Vector Core) into the dmPFC (AP: +3.2; ML: +0.6; DV: -3.5 from skull) at a rate of 1-3 nL/s.

### **Cell density analysis**

Rats unilaterally injected with CtB into the RMTg (n=9) were transcardially perfused with phosphate buffered saline (PBS) followed by 4% paraformaldehyde (PFA). Brains were immersion fixed overnight in 4% PFA, cryoprotected in 30% sucrose, and stored at -80 °C until ready for processing for microscopic analysis. Brains were sliced at 40  $\mu$ m on a cryostat held at -20 °C. Slices containing the PFC and RMTg were labeled for CtB and NeuN using standard immunofluorescence procedures. In brief, slices were incubated in 50% (v/v) methanol for 30 min followed by incubation in 1% H<sub>2</sub>O<sub>2</sub>. Permeabilization was enhanced by incubation in 0.4% Triton-X in PBS followed by incubation in primary antibodies in PBS containing 0.2% Triton-X overnight at 4 °C (CtB 1°: 1:500, List Biological Laboratories #703; NeuN 1°: 1:500, EMD Millipore, MAB377). The tissue was then incubated with secondary antibodies for 2 h at room temperature (1:250, Jackson ImmunoResearch), rinsed in PBS, and mounted onto SuperFrost plus charged slides before being coverslipped with Fluoromount mounting medium (Sigma Aldrich). Images were acquired at 10X and tiled using an EVOS FL Auto microscope. Anatomical boundaries and rostrocaudal level of each PFC slice were determined by aligning the acquired microscopic images with atlas schematics generated using Paxinos & Watson (2007) in GIMP. ImageJ was used to apply a bandpass filter to Fourier-transformed images. For both CtB and NeuN analyses, band-pass filtering was set to the approximate size of a layer V soma, which corresponded to 8-

20 pixels. CtB<sup>+</sup> and NeuN<sup>+</sup> cells were then automatically identified by searching for maximum intensity points with noise tolerance set at 7 and 2 for CtB and NeuN analyses, respectively.

### **Analysis of cell-type**

Adjacent tissue from that used in the cell density analysis experiments (n=3) was used to evaluate whether RMTg-projecting cortical neurons were glutamatergic or GABAergic projection neurons. Slices containing the PFC were labeled for CtB and the glutamatergic marker, CaMKII $\alpha$ , or CtB and the GABAergic marker, GAD67, using the same immunofluorescence procedures described above (CaMKII $\alpha$  1 $^\circ$ : 1:3,000, Invitrogen MA1048; GAD67 1 $^\circ$ : 1:3,000, EMD Millipore MAB5406). Images of labeling in the dmPFC were acquired at 10X using a Zeiss AxioImager.M2 microscope. CtB<sup>-</sup>, CaMKII $\alpha$ <sup>-</sup>, and GAD67-labeled cell bodies were counted manually in each image using ImageJ. Cell counts were averaged across five slices spanning the rostrocaudal extent of the dmPFC for each rat and the ratio of cells labeled with each cell-type marker and CtB relative to all CtB-labeled neurons was calculated.

### **Analysis of collaterals**

A dual-virus, intersectional approach was used to label RMTg-projecting dmPFC neurons. After waiting at least eight weeks for optimal viral transduction and transgene expression, rats were euthanized and brains harvested using the same procedures described above. Brains were sliced on a cryostat at 40  $\mu$ m and eYFP signal was amplified using avidin-biotin immunohistochemistry procedures as previously published (Glover et al., 2016; GFP Abcam, ab290; 1:10,000). Brains were visually inspected from the rostral tip of the PFC to the rostral cerebellum for eYFP<sup>+</sup> terminal labeling. Areas with noticeable labeling were imaged at 10X on a Zeiss AxioImager.M2 microscope. Images were flat field corrected and terminal density was analyzed by measuring the percent-stained area relative to total area using ImageJ. Analysis was performed on four slices spanning the rostrocaudal extent of each region and averaged together to arrive at a single data

point for each region. Analysis of secondary somatosensory cortex and dorsal hippocampus were included as negative controls.

### **Real-time place preference testing**

After at least eight weeks to allow for sufficient viral transduction and transgene expression, rats were tested for real-time place preference using procedures adapted from previously published work (Stamatakis and Stuber, 2012). Rats were habituated to the tethering procedure for at least three days prior to testing. Testing was performed in an unbiased, custom-made apparatus consisting of two contextually distinct compartments. On day one, rats were connected to a patch cable connected to a 473 nm laser and allowed to freely explore the apparatus for 20 min. Light was delivered immediately upon entry into one compartment of the apparatus at 10 mW intensity and 60 Hz for the duration of time spent in that compartment. Light delivery was terminated upon entry into the opposite compartment. To confirm that behavioral responding was light-mediated, rats were re-tested 24 hours later using identical procedures except that the compartment associated with light delivery was reversed. Time spent in each compartment was quantified from video recordings made with a camera mounted above the testing apparatus using Ethovision (Noldus, Leesburg, VA, USA).

### **cFos induction following exposure to foot shocks and tones predictive of foot shock**

cFos induction was measured in RMTg-projecting mPFC neurons following exposure to aversive stimuli using the same procedures as Jhou et al. (2009a). Rats were allowed at least one week to recover following stereotaxic injection of CtB into the RMTg before beginning testing. All rats underwent three days of habituation during which they were tethered and could freely explore a standard operant testing apparatus (Med Associates, St Albans, VT, USA). The house light was illuminated for the duration of each habituation session and all subsequent sessions. On day four, rats in the Context (control) group were euthanized 90 min after an identical 20 min habituation

session. Rats in the Shock group were euthanized 90 min after presentation of a series of 10 foot shocks (0.5 mA, 0.5 s duration, 60 s inter-stimulus interval) over the course of a 20 min testing session beginning 60 s after the start of the session. Rats in the Shock-paired group underwent standard fear conditioning over two consecutive days where tone (2.9 kHz, 65 dB, 20 s duration) presentation co-terminated with foot shock (0.5 mA, 0.5 s duration). Two tone-shock pairings were presented 20 min apart over the course of each 60 min conditioning session. Rats in the Shock-unpaired group were presented with the same stimuli as the Shock-paired group during two 60 min sessions except those stimuli were explicitly unpaired occurring 10 min apart. Following conditioning trials, rats from both the Shock-paired and Shock-unpaired groups were re-habituated to the testing apparatus during a 30 min session where the house light was illuminated but no stimuli were presented. On the test day, rats from both groups were euthanized 90 min after a 20 min test session consisting of presentation of eight tones for 30 s each (60 s inter-stimulus interval). Freezing during tone presentation was scored manually in the Shock-paired and Shock-unpaired rats using overhead video recorded during the test session. Freezing was defined as a complete lack of movement except for respiration. Percent time freezing was calculated as the total amount of time spent freezing during tone presentation relative to the total duration of the tone (30 s). Following euthanasia, brains were processed for CtB (1:300,000) and cFos (Millipore #PC38, 1:10,000) expression using previously published procedures (Glover et al., 2016). The number of double-labeled neurons relative to all CtB+ neurons was quantified manually across 4-5 slices spanning the rostrocaudal extent of the mPFC. Rats with off-target injection sites were excluded from analysis. The total number of cells analyzed as well as average number of cells analyzed per rat for this experiment and those that follow is summarized in **Table S2**.

## **In-situ hybridization**

Rats were unilaterally injected with green retrobeads into the RMTg and allowed at least seven days to recover before testing. The animals were assigned to either Context or Shock groups and underwent testing identical to that described above for the cFos induction experiments. Rats were anesthetized with isoflurane and decapitated 90 min after the test session. The brains were then rapidly removed and placed in ice-cold PBS for ~5 minutes before being embedded in Tissue-Tek OCT media (Sukura Finetek Inc, Torrance, CA, USA) in Peel-A-Way cryo-embedding molds (Polysciences, Inc, Warrington, PA, USA) and covered with dry ice. The frozen tissue block was then extracted from the mold, wrapped in aluminum foil, and stored at -80 °C. Subsequently, 20 µm thick slices from the fresh-frozen brains were cut on a cryostat, mounted on SuperFrost Plus slides (Fisher Scientific, Hampton, NH), and stored at -80 °C until their use in in-situ hybridization experiments.

Fluorescence in-situ hybridization was performed using an Advanced Cell Diagnostics (ACD, Newark, CA) Multiplex RNAScope kit (catalog # 323100). RNA probes for dopamine D1 receptors (catalog # 317031), dopamine D2 receptors (catalog # 315641-C2), and cFos (catalog # 403591-C4) were also obtained from ACD. The RNAScope procedure was carried out according to the manufacturer's instructions (available for download at [www.acdbio.com](http://www.acdbio.com)) with the exception that the protease digestion step was omitted. We observed that omission of this step not only improved the fluorescence intensity of the mRNA transcripts (visually observed as punctate dots), but was also required for preservation of the fluorescent intensity of the green (alexa-488) retrobeads. For multiplex hybridization of D1 and D2 mRNA transcripts, the probes were labeled with Cy3 and Cy5, respectively. For multiplex hybridization of cfos and D1 mRNA transcripts, the probes were labeled with Cy3 and Cy5, respectively. Images were acquired on a Zeiss LSM880 confocal microscope across three PFC slices (5 images/slice) using a 63X oil objective. Imaging was restricted to areas of the dmPFC that exhibited retrograde bead labeling, which was mainly

observed in cortical layer V. Quantification and colocalization of mRNA transcript dot within cells was performed on the captured images using Imaris Software (Bitplane, Zurich, Switzerland) following a previously published method (Centanni et al., 2019). This analysis utilized the Cell Module of Imaris, and can be summarized as follows: 1) Define and interactively threshold the cell nucleus based on DAPI staining (we used a minimum size of 5  $\mu\text{m}$  and a filter of 0.5); 2) Define and interactively threshold the cell body based upon the DAPI identified nucleus in step 1; 3) Define and interactively threshold the mRNA transcript dots for each probe and for the retrobeads (we used a minimum size of 1  $\mu\text{m}$  for both the transcript dots and retrobeads); 4) Calculation of the number and other parameters of the dots that lie within each defined cell. For a cell to be considered as positive for fluorescent beads or D1/D2 mRNA transcripts, it had to contain two or more dots/beads. We observed that a number of cells exhibited a variable level of background cfos mRNA irrespective of whether they were in the Control or Shock group. Therefore, for the purpose of assessment of the effect of shock on cfos mRNA expression, we used a threshold of 15 or more cfos transcript dots in order to consider a cell as being cfos+. This threshold was determined based on a comparison of the distribution of the cfos mRNA transcript dots in the control versus shocked conditions.

### **Whole-cell patch-clamp slice electrophysiology**

Rats were unilaterally injected with green retrobeads into the RMTg and allowed at least three days to recover before being assigned to either Context or Shock groups and undergoing testing identical to that described above for cFos induction experiments. Twenty-four hours following the final day of testing, the intrinsic excitability of dmPFC pyramidal neurons was determined using previously published procedures (Wayman and Woodward, 2018). In brief, rats were anesthetized with urethane (3.0mg/kg, i.p.) and perfused with an ice-cold sectioning solution consisting of (in mM): 200 sucrose, 1.9 KCl, 6 MgSO<sub>4</sub>, 1.4 NaH<sub>2</sub>PO<sub>4</sub>, 25 NaHCO<sub>3</sub>, 0.5 CaCl<sub>2</sub>, 10 glucose, and 0.4 ascorbic acid; pH 7.35-7.45 with 310-320 mOsm. The brains were then immediately harvested

and coronal brain sections (300  $\mu\text{m}$ ) containing the dmPFC were sliced on a Leica VT1000S vibratome (Leica Biosystems, Buffalo Grove, IL) in oxygenated (95%  $\text{O}_2$ ; 5%  $\text{CO}_2$ ) sectioning solution and then transferred to a holding chamber containing normal artificial cerebrospinal fluid (aCSF; in mM): 125 NaCl, 2.5 KCl, 25  $\text{NaHCO}_3$ , 1.4  $\text{NaH}_2\text{PO}_4$ , 1.3  $\text{MgCl}_2$ , 2  $\text{CaCl}_2$ , and 10 glucose; pH 7.35-7.45 with 310-320 mOsm. Brain slices were incubated at 34  $^\circ\text{C}$  for 30 minutes and allowed to recover at room temperature for an additional 45 minutes.

For current clamp recordings, brain slices were transferred to the recording chamber and perfused with oxygenated and heated ( $\sim 34$   $^\circ\text{C}$ ) aCSF at a flow rate of 2 mL/min. The temperature was maintained during the course of the recordings with in-line and bath heaters (Warner Instruments, Hamden, CT). Retrobead-labeled layer V neurons within the dmPFC were visually identified using a Zeiss FS2 microscope (Zeiss, Thorndale, NY). Recording pipettes were constructed from thin-walled borosilicate capillary glass tubing (I.D.=1.17mm, O.D. 1.50mm; Warner Instruments, Hamden, CT), pulled with a horizontal pipette puller (P-97 Sutter Instrument Co., Novata, CA). Pipettes were filled with an internal solution containing (in mM): 120 K-gluconate, 10 HEPES, 10 KCl, 2  $\text{MgCl}_2$ , 2  $\text{Na}_2\text{ATP}$ , 0.3  $\text{NaGTP}$ , 1 EGTA and 0.2% biocytin; pH 7.35-7.45 with 285-295 mOsm and had resistances ranging from 3-5  $\text{M}\Omega$ . After a stable gigaohm seal was formed, light suction was applied to break through the cell membrane and achieve whole-cell access. Neurons with an access resistance of greater than 20  $\text{m}\Omega$  were not used for analysis. Recorded events were acquired with an Axon MultiClamp 700A amplifier (Molecular Devices, Union City, CA), digitized at a sampling rate of 10 kHz (filtered at 4 kHz) with an Instrutech ITC-18 analog-digital converter (HEKA Instruments, Bellmore, NY) controlled by AxographX software (Axograph Scientific, Sydney, Australia) running on a Macintosh G4 computer (Apple, Cupertino, CA). The resting membrane potential (RMP) and capacitance of all neurons was first recorded and then the RMP was adjusted to -70 mV for electrophysiological assessments of excitability. Action potential firing was induced by a series of 500 ms current steps (0-300 pA) incremented in +20



pA steps. Recordings were analyzed offline for the number of spikes in response to each current step, threshold (mV), rheobase (pA), action potential peak amplitude (mV), action potential half-width (ms) and after-hyperpolarization (AHP; mV) using AxographX software.

The caudal portion of the brain containing the RMTg was collected at the same time that dmPFC slices were generated, immersion fixed overnight in 4% PFA, and frozen on dry ice followed by storage at -80 °C until processing. Injection sites were confirmed by visual inspection of fluorescent retrobead labeling in slices containing the RMTg made using a cryostat.

### **Spine density analysis**

A dual-virus, intersectional approach was used to label RMTg-projecting dmPFC neurons. After waiting at least eight weeks for optimal viral transduction and transgene expression, rats were assigned to either Context or Shock groups and underwent behavioral testing identical to that described above for cFos induction experiments. Twenty-four hours later, rats were euthanized, and brains harvested as described for cell density analysis. Brains were sliced at 100  $\mu\text{m}$  and eYFP signal was amplified (GFP, Abcam #ab290; 1:30,000) using immunofluorescence procedures optimized for thick slices (Kupferschmidt et al., 2015). Primary apical dendrites measuring 55  $\mu\text{m}$  in length approximately 200-300  $\mu\text{m}$  from the soma of eYFP+ neurons in the dmPFC were imaged using a 63.5X oil immersion objective on a Zeiss LSM880 confocal microscope. Images were analyzed in Imaris using previously published procedures (McGuier et al., 2015). Dendrite diameter, dendrite volume, and total spine density were analyzed in addition to analyses conducted by spine classification. Measures included density, length, diameter, and volume by spine class as well as diameter and volume of spine terminal point and spine neck volume, length, and diameter. Measures were collected in 3-5 dendrites per rat and averaged across dendrites to arrive at a single value for each rat.

## SUPPLEMENTARY RESULTS

### Collaterals

Quantification of punctate staining revealed the greatest density of collaterals in the dorsomedial striatum ( $11.31 \pm 3.11\%$ ), whereas the dorsolateral striatum was virtually devoid of labeling ( $0.07 \pm 0.01\%$ ). Ventrally, RMTg-projecting dmPFC neurons collateralized to a moderate degree in the nucleus accumbens core ( $6.03 \pm 1.31\%$ ) as well as the shell ( $0.34 \pm 0.19\%$ ), albeit very weakly. Substantial collateralization was also observed in the ventral pallidum ( $11.05 \pm 3.98\%$ ), hypothalamus ( $8.48 \pm 0.98\%$ ), periaqueductal gray ( $6.54 \pm 1.50\%$ ), and lateral preoptic nucleus ( $6.20 \pm 0.74\%$ ). Terminal labeling was much less dense in the lateral habenula ( $5.15 \pm 1.55\%$ ) and ventral tegmental area ( $2.58 \pm 1.07\%$ ) – two regions heavily interconnected with both the dmPFC and the RMTg. By comparison, terminal labeling in the RMTg itself was  $3.58 \pm 0.17\%$ . The amygdala also receives significant input from layer V dmPFC neurons and, like the RMTg, is well-known for its role in avoidance and aversive signaling. Despite this, only very weak terminal labeling was apparent in this region ( $0.94 \pm 0.08\%$ ). The dorsal hippocampus (Hipp) and secondary somatosensory cortex (S2) were used as negative controls as it is well-known that these regions do not receive any input from the dmPFC (Hipp:  $0.02 \pm 0.01\%$ ; S2:  $0.01 \pm 0.00\%$ ).

### **cFos, D1, D2 mRNA expression following exposure to repeated foot shock**

FigureS2 shows an expanded analysis of the data presented in Figure 2 of the main manuscript. D1 and D2 mRNA analysis was performed in Context- and Shock-exposed rats. Fluorescent retrobead-labeled cells (bead+) comprised approximately 62% of the total population of cells analyzed. A two-way ANOVA indicated that there was no significant difference in the number of either total or bead+ cells between control and shock-exposed rats [Main effect of treatment:  $F(1,12)=0.002$ ,  $p=0.0966$ ; treatment x cell-type:  $F(1,12)=0.10$ ,  $p=0.759$ ] (**Figure S2A**). In addition, no significant between-group differences were observed using a two-way ANOVA to compare the

percent of bead+ cells that were also positive for either D1 or D2 mRNA in control and shock-exposed rats [ $F(3,24)=0.28$ ,  $p=0.8411$ ] (**Figure S2B**).

To examine whether exposure to an aversive stimulus altered the magnitude of dopamine receptor gene expression in RMTg-projecting dmPFC neurons, two-way ANOVAs were used to compare the average number of RNAScope dots present per cell across dopamine receptor-expressing cell types. As shown in **Figures S2C-D**, foot shock exposure had no significant effect on either D1 (Treatment:  $F(1,18)=2.09$ ,  $p=0.1651$ ; treatment x cell-type:  $F(2,18)=0.21$ ,  $p=0.8138$ ) or D2 (Treatment:  $F(1,18)=1.38$ ,  $p=0.2550$ ; treatment x cell-type:  $F(2,18)=0.30$ ,  $p=0.7445$ ) mRNA expression.

To further explore whether cFos induction observed following exposure to aversive stimuli is specific to a unique dopamine receptor-expressing population of dmPFC-RMTg neurons, we measured induction of cfos mRNA colocalized with D1 receptor mRNA (the predominantly expressed dopamine receptor in these neurons). As expected, cfos expression was significantly enhanced in Shock-exposed rats relative to rats exposed to a neutral context (**Figure S3A**), and this was true regardless of retrobead labeling [two-way ANOVA main effect of treatment:  $F(1,12)=4.72$ ,  $p=0.0505$ ]. When comparing cfos expression in D1<sup>+</sup> and D1<sup>-</sup> RMTg-projecting dmPFC neurons, a two-way ANOVA revealed a main effect of treatment with Shock-exposed rats exhibiting a greater proportion of cfos in both cell types relative to Context controls (**Figure S3B**). However, this effect only trended toward statistical significance for a main effect of shock exposure [ $F(1,12)=4.05$ ,  $p=0.0673$ ]. Similarly, the magnitude of cFos mRNA expression, as measured by average number of cFos dots per cell, was significantly greater in RMTg-projecting dmPFC neurons of Shock-exposed rats compared to controls regardless of D1 receptor expression profile (**Figure S3C**; main effect:  $F(1,12)=4.50$ ,  $p=0.0555$ ). Altogether, these data indicate that RMTg afferents arising in the dmPFC are highly enriched in D1 dopamine receptors

(with D2 receptors colocalized to many of these neurons), and that the effects of exposure to aversive stimuli are similar across dmPFC-RMTg neurons with differing dopamine receptor expression profiles.

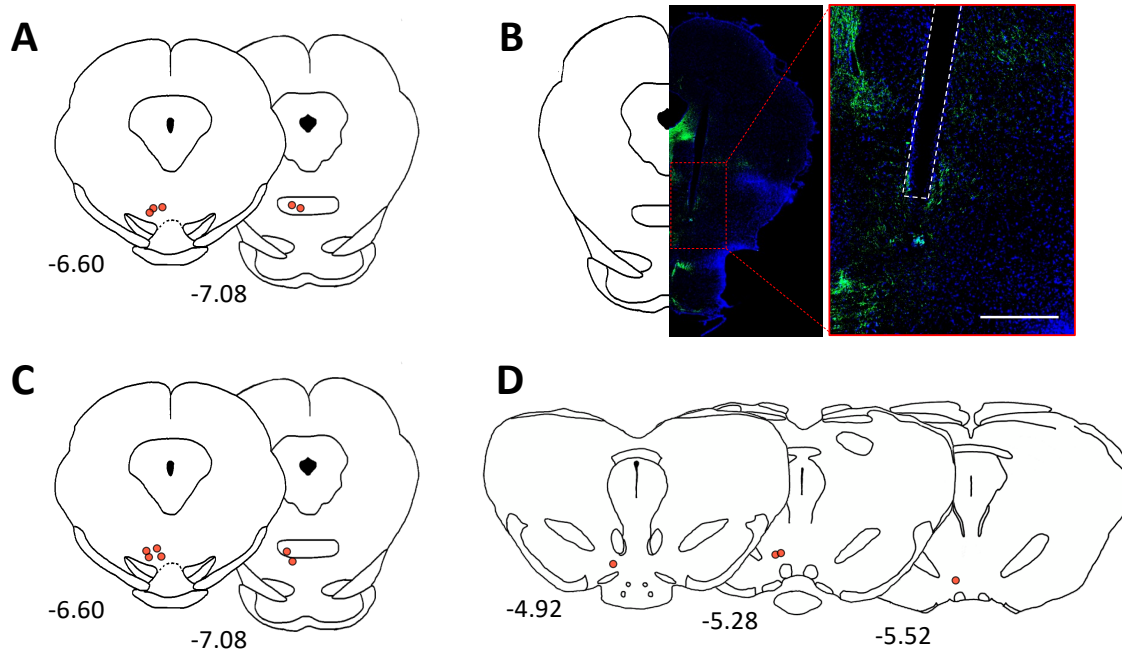


**Figure S1. Implant sites for RTPP optogenetics experiment. (A)** Implant termination sites for PL-RMTg group. **(B)** Representative image of GFP-labeled PL terminals in the RMTg and implant tract (outlined in white) in a rat from the PL-RMTg group. **(C)** Implant termination sites for Lhb-RMTg group. **(D)** Implant termination sites for PL-VTA group. Scale = 500  $\mu$ M.

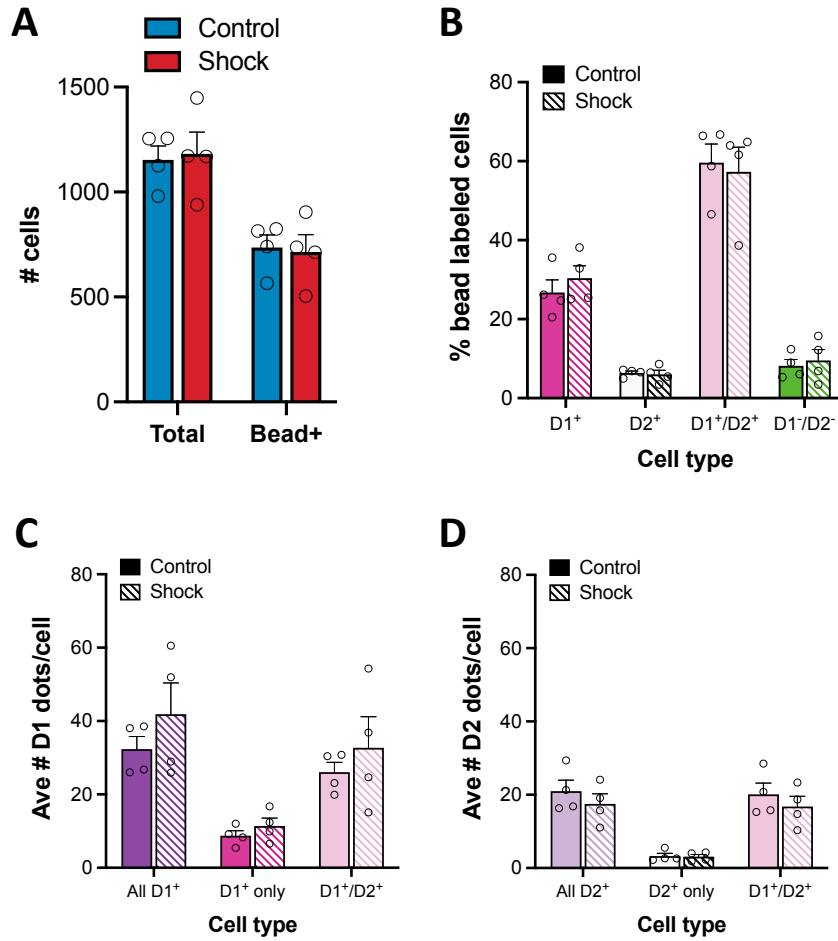


**Figure S2. D1 & D2 receptor gene expression in RMTg-projecting dmPFC neurons from context- and shock-exposed rats.** These data are the same as what is depicted in Figure 2 of the main manuscript but broken down by shock and context control groups. **(A)** Foot shock had no effect on the total number of cells or number of bead positive cells analyzed. **(B)** The prevalence of D1 and D2 mRNA transcript containing cells was similar between the treatment groups with the majority of RMTg-projecting dmPFC neurons being D1<sup>+</sup> and a large proportion also expressing D2 receptor mRNA. Foot shock exposure had no significant effect on the magnitude of either D1 **(C)** or D2 **(D)** mRNA expression.

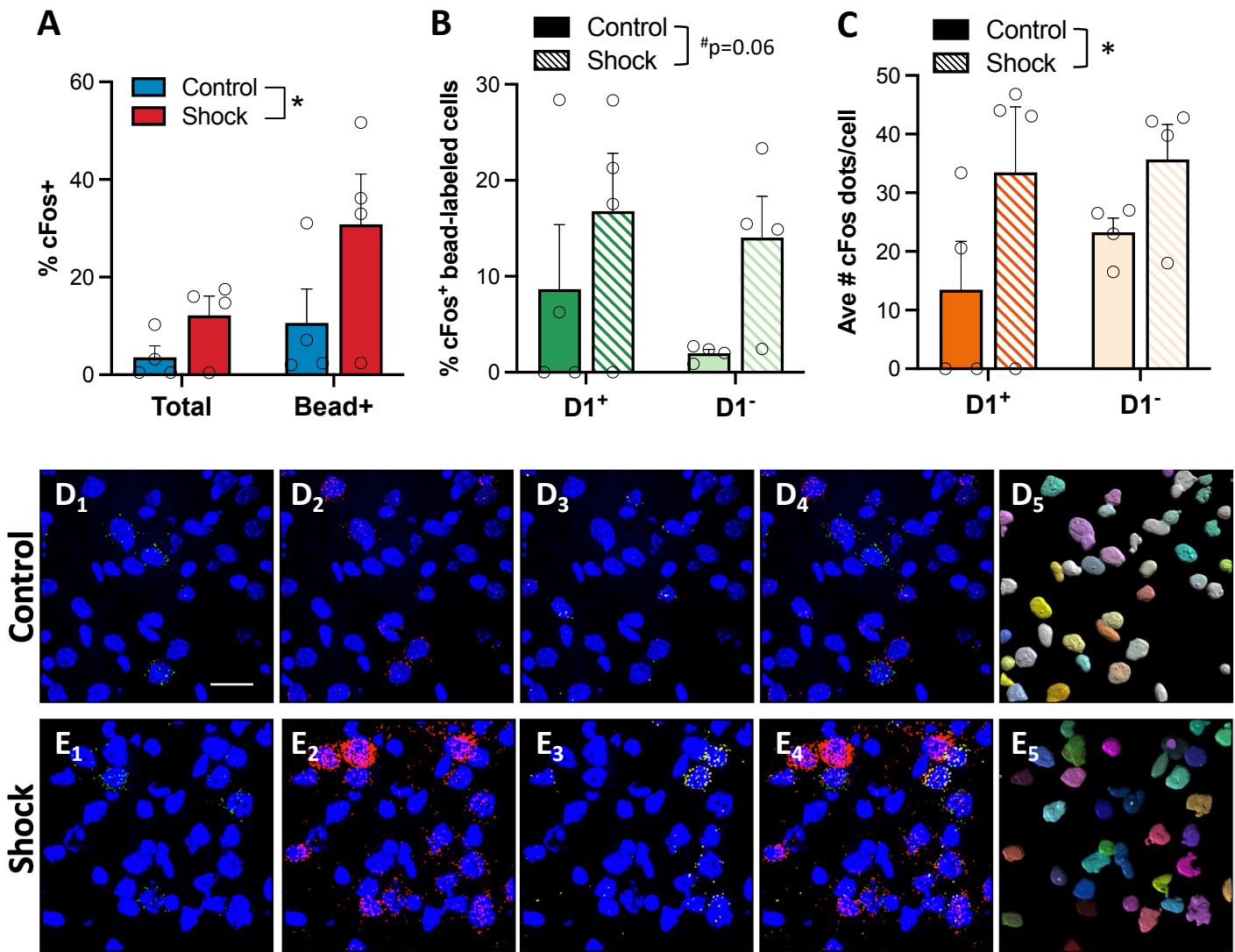


**Figure S3. Shock-induced enhancement of cFos expression occurs in both D1<sup>+</sup> and D1<sup>-</sup> RMTg-projecting dmPFC neurons.** (A) Shock exposure significantly increased cFos mRNA expression in both bead<sup>+</sup> and bead<sup>-</sup> dmPFC neurons. (B) cFos expression was similarly increased in both D1<sup>+</sup> and D1<sup>-</sup> neurons in shock-exposed rats relative to controls. (C) cFos mRNA expression was significantly greater in shock-exposed rats compared to controls, but there was no significant difference between D1<sup>+</sup> and D1<sup>-</sup> cell populations. Representative RNAScope labeling from a context-exposed control (D) and shock-exposed (E) rat. Retrobead labeling is depicted in green (D-E<sub>1</sub>), cFos mRNA in red (D-E<sub>2</sub>), D1 receptor mRNA in yellow (D-E<sub>3</sub>), merged image (D-E<sub>4</sub>) and IMARIS rendering of colocalized beads and dots the cell soma (D-E<sub>5</sub>). Nuclear labeling by DAPI depicted in blue. Scale bar = 20  $\mu$ m; \* $p$ ≤0.05.

Measure	Statistical test	Effect	Result
Dendrite diameter	Unpaired t-test		t(10)=0.6430, p=0.3960
Dendrite volume	Unpaired t-test		t(10)=0.3731, p=0.1613
Overall spine density	Unpaired t-test		t(10)=0.2997, p=0.4101
Spine density by class	Two-way ANOVA	Class	<b>F(3,40)=53.37, p&lt;0.0001</b>
		Treatment	F(1,40)=0.0750, p=0.7856
		Class x Treatment	F(3,40)=1.338, p=0.2756
Spine length by class	Two-way ANOVA	Class	<b>F(3,36)=224.7, p&lt;0.0001</b>
		Treatment	F(1,36)=1.427, p=0.2401
		Class x Treatment	F(3,36)=1.573, p=0.2129
Spine diameter by class	Two-way ANOVA	Class	<b>F(3,36)=23.77, p&lt;0.0001</b>
		Treatment	F(1,36)=2.492, p=0.1232
		Class x Treatment	F(3,36)=0.8049, p=0.4994
Terminal point diameter by class	Two-way ANOVA	Class	<b>F(3,36)=13.77, p&lt;0.0001</b>
		Treatment	F(1,36)=0.0579, p=0.8112
		Class x Treatment	F(3,36)=0.0967, p=0.9614
Spine volume by class	Two-way ANOVA	Class	<b>F(3,36)=15.89, p&lt;0.0001</b>
		Treatment	F(1,36)=1.832, p=0.1843
		Class x Treatment	F(3,36)=0.7693, p=0.5188
Spine neck volume by class	Two-way ANOVA	Class	<b>F(3,36)=18.86, p&lt;0.0001</b>
		Treatment	F(1,36)=2.404, p=0.1298
		Class x Treatment	F(3,36)=0.9704, p=0.4173
Terminal point volume by class	Two-way ANOVA	Class	<b>F(3,36)=5.712, p=0.0026</b>
		Treatment	F(1,36)=0.9216, p=0.3435
		Class x Treatment	F(3,36)=0.6379, p=0.5955
Neck length by class	Two-way ANOVA	Class	<b>F(3,29)=180.6, p&lt;0.0001</b>
		Treatment	<b>F(1,29)=4.190, p=0.0498</b>
		Class x Treatment	<b>F(3,29)=3.179, p=0.0388</b>
Neck diameter by class	Two-way ANOVA	Class	<b>F(3,33)=27.33, p&lt;0.0001</b>
		Treatment	<b>F(1,33)=9.847, p=0.0036</b>
		Class x Treatment	F(3,33)=1.689, p=0.1884

**Table S1. Complete analysis of dendritic spine density & morphology in RMTg-projecting dmPFC neurons following exposure to aversive stimuli.** Bolded results indicate statistical significance of  $p \leq 0.05$ .



<b>Experiment</b>	<b># cells analyzed</b>	<b>Ave # cells analyzed/rat</b>
Figure1D-G		
CtB	22,770	2,530 ± 281.30
NeuN	291,113	32,346 ± 2,661.10
Figure2A-D		
CaMKIIa	990	330 ± 14.22
GAD67	843	281 ± 26.08
Figure 2E-H	9,342	1,168 ± 57.17
Figure 4	48,210	1,269 ± 48.59
Figure 5A-K	23	1.92 ± 0.23
Figure 5L-P	44	3.67 ± 0.31

**Table S2. Total and average number of cells per rat analyzed for each experiment.**